High pressure evolution of $YVO_4:Pr^{3+}$ luminescence

2009 J. Phys.: Condens. Matter 21 105401

(http://iopscience.iop.org/0953-8984/21/10/105401)

J. Phys.: Condens. Matter **21** (2009) 105401 (7pp) doi:10.1088/0953-8984/21/10/105401

High pressure evolution of $YVO_4:Pr^{3+}$ luminescence

S Mahlik[1], M Grinberg[1], E Cavalli[2], M Bettinelli[3] and P Boutinaud[4]

[1] Institute of Experimental Physics, University of Gdańsk, Wita Stwosza 57, 80-952 Gdańsk, Poland
[2] Dipartimento di Chimica Generale ed Inorganica, Chimica Analitica, Chimica Fisica, Università di Parma, 43100 Parma, Italy
[3] Dipartimento Scientifico e Tecnologico, Università di Verona, and INSTM, UdR Verona, 37134 Verona, Italy
[4] Laboratoire des Matériaux Inorganiques, Université Blaise-Pascal, 63177 Aubière, France

Received 23 October 2008, in final form 2 January 2009
Published 13 February 2009
Online at stacks.iop.org/JPhysCM/21/105401

Abstract
Photoluminescence and time-resolved photoluminescence spectra of YVO_4 doped with Pr^{3+} obtained at high hydrostatic pressure up to 76 kbar applied in a diamond anvil cell are presented. At pressures lower than 60 kbar the steady state emission spectra consist of sharp lines related to the $^1D_2 \rightarrow {}^3H_4$ transition in Pr^{3+}. At pressures above 68 kbar the Pr^{3+} emission intensity decreases and the corresponding bands are replaced by a broad band peaking at 19 500 cm^{-1} attributed to perturbed VO_4^{3-} host luminescence. The quenching of the $^1D_2 \rightarrow {}^3H_4$ emission has been attributed to nonradiative transition to the charge transfer exciton trapped at Pr^{3+} ion. The recovering of the VO_4^{3-} host luminescence at high pressure has been attributed to energy transfer from a Pr^{3+} trapped exciton (PTE) to the host YVO_4. The kinetics of such a process is analyzed using the model of PTE considered as a Pr^{4+} + electron bound by the Coulomb potential at the delocalized Rydberg states.

1. Introduction

The host dependence of luminescence of praseodymium-doped oxide materials is related to the possibility of forming Pr^{3+} trapped charge transfer exciton states, also called intervalence charge transfer (IVCT) states (Boutinaud *et al* 2005, 2006a, 2006b). Specifically it has been shown that these states, depending on their energies, are responsible for the quenching of the blue luminescence related to the Pr^{3+} spin allowed $^3P_0 \rightarrow {}^3H_4$ transition, (Boutinaud *et al* 2006b). A model of formation of such states has been proposed by Reut and Ryskin (1973) as the transfer of electrons from Pr^{3+}, whose fourth ionization potential is relatively low, to a reducible lattice cation M^{n+} and the consequent formation of a $Pr^{4+} + M^{(n-1)+}$ system. The alternate model of a Pr^{3+} trapped exciton (PTE) has been proposed by Gryk *et al* (2006) where one deals with Pr^{4+} and an electron bound by a long range Coulomb potential at quasi-shallow donor states.

Boutinaud *et al* (2006b), (2007) have analyzed the energy of the IVCT states as a function of the optical electronegativity of the d^0 lattice cation and the Pr^{3+}–nearest cation distance. A decrease of energy of the IVCT state has been found with increasing electronegativity. According to the data collected in Boutinaud *et al* (2007), this energy also decreases with decreasing lattice constant. Systematic investigations of the Pr^{3+} luminescence in $LiTaO_3:Pr^{3+}$ and $LiNbO_3:Pr^{3+}$ under high hydrostatic pressure (Gryk *et al* 2005a, 2006, 2005b, 2004) reveal that the energy of the PTE decreases with increasing pressure. In the case of $LiNbO_3:Pr^{3+}$ (Gryk *et al* 2005a, 2004) the PTE state is located between the $^1D_2$ and $^3P_0$ states of Pr^{3+} and therefore in ambient conditions only $^1D_2$ luminescence is observed. The pressure decreases the energy of the PTE state below $^1D_2$, giving rise to quenching of the $^1D_2 \rightarrow {}^3H_4$ luminescence. In the case of $LiTaO_3:Pr^{3+}$, (Gryk *et al* 2006, 2005b) the PTE energy is higher than that of $^3P_0$. Therefore at ambient conditions both transitions originating from $^1D_2$ and $^3P_0$ contribute to the luminescence. Pressure decreases the energy of PTE and causes the quenching of the $^3P_0$ emission.

It should be pointed out that the different labels IVCT and PTE refer to the same phenomenon, which is related to ionization of Pr^{3+} to Pr^{4+}. The differences concern the localization of the electron. In CTS and IVCT the electron is considered as localized at the nearest cation, whereas in

PTE it is delocalized at quasi-shallow donor states. Actually, an infinite Coulomb potential has always localized Rydberg states, and the only problem is if these states can be stable in dielectric crystals and participate in the luminescence processes, or the electron is finally localized at another lattice cation as is predicted by the IVCT model.

In this paper we present the evolution of the luminescence of the YVO_4:Pr^{3+} system as a function of pressure. In ambient conditions, the PTE state is located between the $^1D_2$ and $^3P_0$ states of Pr^{3+}. Pressure causes the quenching of the $^1D_2 \rightarrow {}^3H_4$ emission; however, this is accompanied by recovery of the VO_4^{3-} emission. We discuss this effect using the PTE model and show that the delocalization of an electron at Rydberg states is important for an effective energy transfer from the PTE to the VO_4^{3-} molecular ion.

2. Experimental details

YVO_4 crystals doped with 1 mol% Pr^{3+} were grown as described in Boutinaud *et al* (2004). High pressure was applied in a diamond anvil cell (DAC) of the Merrill–Bassett type (Merrill and Bassett 1974); poly(dimethylsilloxane) oil was used as the pressure transmitting medium and a ruby crystal has been used as pressure sensor. Steady state luminescence was excited with an He–Cd laser with wavelength 325 nm. Luminescence was dispersed by a PGS2 spectrometer working as a monochromator and detected by an R943-2 photomultiplier working in the photon counting regime. The experimental set-up for luminescence kinetics and time resolved spectroscopy was described in detail in Kubicki *et al* (2006). The set-up consists of an OPG system that generates 30 ps laser pulses of 335 nm wavelength, with frequency 10 Hz, a spectrometer and a Hamamatsu Streak Camera model C4334-0. The time resolved luminescence spectra were collected by integration of the streak camera pictures over the time intervals, whereas the luminescence decays were collected by integration of the streak camera pictures over the wavelength intervals. Luminescence excitation spectra were measured using a system consisting of an Xe lamp (450 W), two monochromators SPM2 (one in the excitation and one in the detection line) and two photomultipliers (the first for the luminescence and the second for reference signal detection). All spectra have been measured at ambient temperature.

3. Results

Luminescence and luminescence excitation spectra of YVO_4:Pr^{3+} are presented in figure 1. The luminescence spectrum (solid curve) consists of sharp emission lines peaking at 16 180, 16 455, 16 500 and 16 800 cm^{-1}, related to $^1D_2 \rightarrow {}^3H_4$ transitions in the Pr^{3+} ion, a sharp line peaking at 17 400 cm^{-1} related to Dy^{3+} impurity luminescence and a broad band peaking at 22 500 cm^{-1} related to VO_4^{3-} emission, (Blasse 1980). Excitation spectra of the Pr^{3+} luminescence monitored at 16 500 cm^{-1} (dashed curve) consists of three sharp lines peaking at 19 840 cm^{-1}, 20 470 cm^{-1} and 21 640 cm^{-1} related to transitions from the ground state $^3H_4$ to the excited

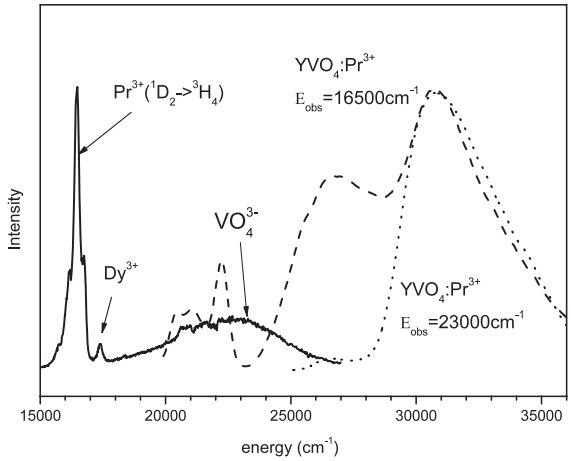

Figure 1. Luminescence (solid curve) and luminescence excitation spectra of YVO_4:Pr^{3+}. Excitation spectrum of the emission monitored at 16 500 cm^{-1} and 23 000 cm^{-1} is presented by a dashed curve and dotted curve, respectively.

states $^3P_0$, $^3P_1$ and $^3P_2$ states of Pr^{3+}, respectively. One observes additionally two broad bands peaked at 26 800 and 30 500 cm^{-1}. A similar two-band structure in the $^1D_2 \rightarrow {}^3H_4$ luminescence excitation spectra has been observed in other vanadates and titanates containing Pr^{3+} (Boutinaud *et al* 2006a) and has been attributed to the intervalence charge transfer state (the band at lower energy) and an internal transition in vanadate or titanate complexes (the band at higher energy). Similar bands in the $^1D_2 \rightarrow {}^3H_4$ luminescence excitation spectra in Pr^{3+}-doped $LiNbO_3$ crystals, observed by Koepke *et al* (2006), have been related to the Pr^{3+} trapped exciton (PTE). We consider that, in the YVO_4:Pr^{3+} crystal investigated in this paper, the band peaking at 26 800 cm^{-1} is related to the PTE state, whereas the band peaking at 30 500 cm^{-1} can be related to absorption in the VO_4 complex. The excitation spectrum of the VO_4^{3-} emission, monitored at 23 000 cm^{-1} (dotted curve), consists mainly of the band peaking at 30 500 cm^{-1} and a hump peaking at 26 800 cm^{-1}.

Luminescence spectra of YVO_4:Pr^{3+} obtained at different pressures are presented in figure 2(a). One observes the redshifts of the emission lines related to $^1D_2 \rightarrow {}^3H_4$ transitions that are -2.3 cm^{-1} $kbar^{-1}$, -1.7 cm^{-1} $kbar^{-1}$, -1.4 cm^{-1} $kbar^{-1}$ and -1.0 cm^{-1} $kbar^{-1}$ for the lines peaking at 16 180 cm^{-1}, 16 455 cm^{-1}, 16 500 cm^{-1} and 16 800 cm^{-1}, respectively. Positions of the peaks related to $^1D_2 \rightarrow {}^3H_4$ transitions versus pressure are presented in figure 2(b). The energy of the Dy^{3+} luminescence is almost pressure-independent. One observes also that the intensities of the $^1D_2 \rightarrow {}^3H_4$ and of the Dy^{3+} luminescence decrease with increasing pressure. In figure 2(a) normalized spectra are presented and therefore this effect is not noticed. The effect of $^1D_2 \rightarrow {}^3H_4$ luminescence quenching with increasing pressure has been observed in Pr^{3+}-doped $LiNbO_3$ (Gryk *et al* 2005a, 2006) and has been attributed to a decrease of the energy of the PTE state with respect to the $^1D_2$ state of Pr^{3+}. In $LiNbO_3$:Pr^{3+} the decrease of the intensity of the $^1D_2 \rightarrow {}^3H_4$ transition with pressure has been found to be accompanied by the appearance

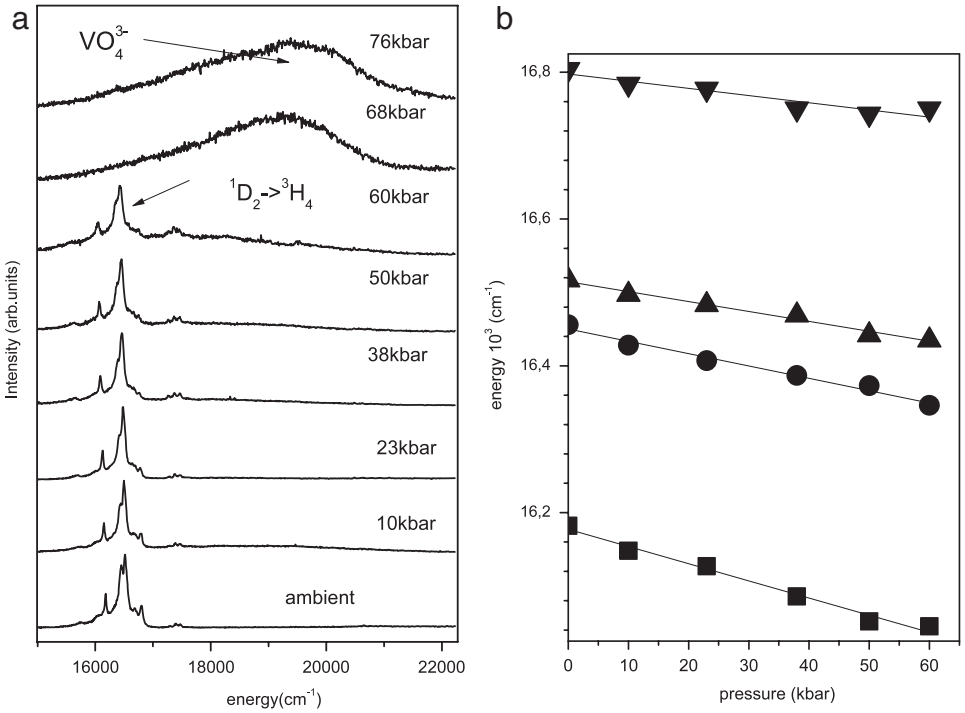

Figure 2. (a) Luminescence spectra of YVO_4:Pr^{3+} at different pressures. (b) Energies of peaks related to $^1D_2 \rightarrow {}^3H_4$ transitions in Pr^{3+} versus pressure.

of the broad band emission shifted strongly to the red. As seen in figure 2(a), the quenching of the $^1D_2 \rightarrow {}^3H_4$ emission in YVO_4:Pr^{3+} is accompanied by the appearance of a broad band luminescence peaking at 19 500 cm^{-1}. This luminescence can be attributed to emission of VO_4^{3-} ions close to defects (Polosan *et al* 2007). At pressures above 68 kbar and higher the Pr^{3+} and Dy^{3+} emission is replaced by a broad band emission related to VO_4^{3-} located close to defects.

Contributions of the VO_4^{3-} band, Pr^{3+} and Dy^{3+} luminescence to the whole spectrum of YVO_4:Pr^{3+} are analyzed by time resolved spectroscopy. In figure 3 time resolved luminescence spectra of YVO_4:Pr^{3+} are presented. Different time intervals are indicated in figure 3. One can see that Dy^{3+} emission (the lines centered at 17 400 and 20 800 cm^{-1}) is the most persistent one. The spectrum obtained in the time interval 0–10 μs is Interesting. Apart from the Pr^{3+} luminescence the fast decaying emission band related to VO_4^{3-} is observed. VO_4^{3-} emission has been observed many times (Ryba-Romanowski 2003, Boutinaud *et al* 2004, 2007) in undoped YVO_4 and in YVO_4:Pr^{3+}. It has been shown (Boutinaud *et al* 2004) that the VO_4^{3-} luminescence lifetime decreases (i.e. it is accompanied by a decrease in its intensity) when the material is doped with Pr^{3+}. This effect can be interpreted as related to nonradiative energy transfer from the VO_4^{3-} to Pr^{3+} ion. We have found that, at ambient pressure, the intensity of the VO_4^{3-} band relative to the Pr^{3+} emission depends on the excitation energy and increases when we excite the system with photons of higher energy (see the excitation spectra in figure 1). The presence of the emission related to the perturbed VO_4^{3-} system at high pressure means that the excitation energy transfer from the VO_4^{3-} to Pr^{3+} ion is not

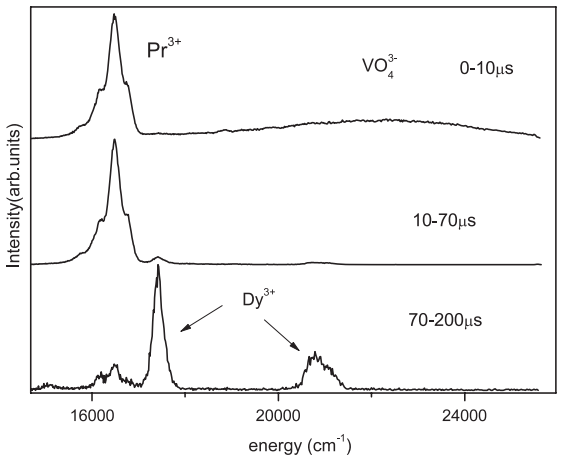

Figure 3. Time resolved luminescence spectra of YVO_4:Pr^{3+} obtained at ambient pressure.

active at high pressure and is replaced by the reverse energy transfer from the Pr^{3+} ion to the VO_4^{3-} molecular ions.

In figure 4(a) the decays of the Pr^{3+} emission related to the $^1D_2 \rightarrow {}^3H_4$ transition at different pressures are presented. For pressures below 42 kbar the decay is exponential and the decay constant decreases from 12.5 μs for ambient pressure to 4.0 μs for 42 kbar.

The decrease of the $^1D_2$ lifetime is accompanied by luminescence quenching. The same effect has been observed in Pr^{3+}-doped $LiNbO_3$ (Gryk *et al* 2006) and has been related to the de-excitation of the $^1D_2$ state through the PTE recombination.

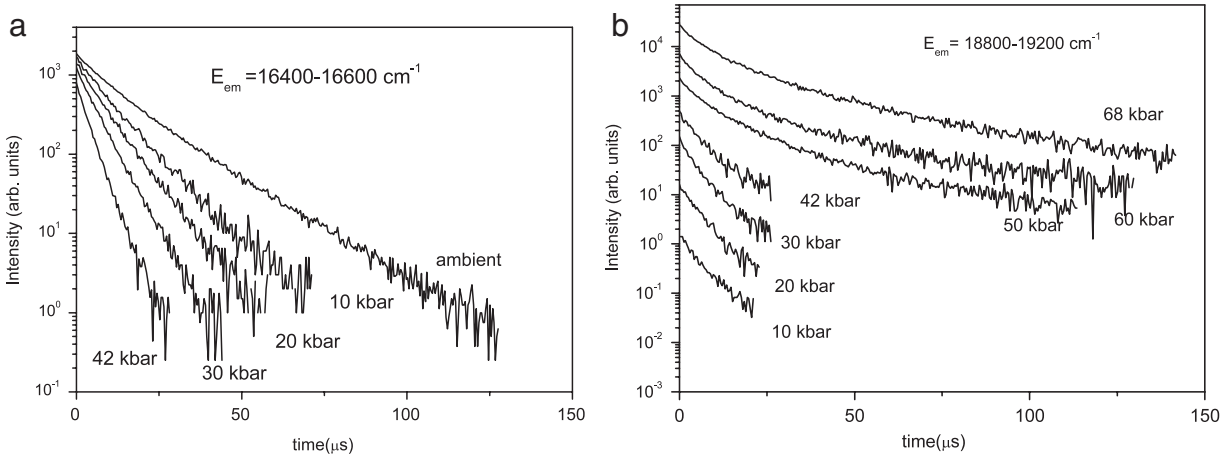

Figure 4. (a) Decay of the Pr^{3+} emission related to the $^1D_2 \rightarrow {}^3H_4$ transition at different pressures, (b) decay of the perturbed YVO_4 host emission for different pressure.

The decays of the luminescence corresponding to the perturbed VO_4^{3-} emission are presented in figure 4(b). The decays are multi-exponential and become longer for higher pressure. For pressures below and above 50 kbar, the average lifetime of the band calculated as $\tau = \int tI(t)\,dt / \int I(t)\,dt$ is approximately equal to 5 μs and 15 μs, respectively. A time constant $\tau = 15$ μs is very close to 14 μs obtained for the VO_4^{3-} host emission in undoped YVO_4 (Boutinaud *et al* 2004). The multi-exponential decay of the host luminescence can be related to inhomogeneous properties of the VO_4^{3-} complex, the distance from Pr^{3+}, the existence of other defects and amorphization of the material. The influence of other defects and amorphization can be increased by pressure.

The recovering of the VO_4^{3-} emission at high pressure, the lifetime variations of the $^1D_2 \rightarrow {}^3H_4$ emission and the VO_4^{3-} emission versus pressure indicate that, although the decrease of the $^1D_2 \rightarrow {}^3H_4$ luminescence lifetime can still be related to nonradiative retransfer of the excitation energy from the $^1D_2$ state of Pr^{3+} to the PTE state, further relaxation of the system is not the nonradiative recombination of the Pr^{3+} trapped exciton. To analyze the possible relaxation pathways we consider the PTE model proposed in Gryk *et al* (2006) for the $LiNbO_3$:Pr^{3+} system and developed by Grinberg and Mahlik (2008).

4. Model of impurity-trapped exciton

In order to analyze the processes of trapping free carriers at the Pr^{3+} center we have considered the energetic structure of the system presented in figure 5(a). E_1 and E_2 represent the energy of internal transition in the impurity ($^3H_4 \rightarrow {}^1D_2$) and $Pr^{3+} \rightarrow Pr^{4+}$ ionization energy, respectively. E_3 is the energy released when a free hole from the valence band is captured by Pr^{3+} (as the result the Pr^{4+} ion is created). To describe the system of a Pr^{4+} ion and an electron in the conduction band more quantitatively the following Hamiltonian has been proposed (Gryk *et al* 2005b):

$$H = \frac{-\hbar^2\nabla^2}{2m} + V_{cr}(\mathbf{r})|_{r>R} + V_{RE}(\mathbf{r})|_{r<R} - \frac{e^2}{\varepsilon r} + V_{latt}(\Delta, \mathbf{r}). \tag{1}$$

In relation (1) $V_{RE}(\mathbf{r})$ is the local potential of the rare earth ion and $V_{cr}(\mathbf{r})$ is the lattice periodic potential. The subscripts $r > R$ and $r < R$ denote the potential outside and inside the first coordination sphere, respectively, while R is the average distance between the Pr^{4+} ion and O^{2-} ligands. A hole localized at Pr^{3+} (i.e. Pr^{4+}) creates a long range Coulomb potential, $-\frac{e^2}{\varepsilon r}$.

The Hamiltonian (1) generates two types of bound states: the localized states related to the short range potential $V_{RE}(\mathbf{r})$ that originates from the Pr^{3+} ($4f^2$ electronic configuration) energetic structure and the delocalized states of the shallow donor type (the Rydberg states) that are related to the long range potential $-\frac{e^2}{\varepsilon r}$ of the Pr^{4+} ion. The electron ionization energy of an electron at the lowest Rydberg state is given by the effective Rydberg quantity:

$$\mathrm{Ry}^* = -13.6\frac{m_e^*}{\varepsilon^2}eV \tag{2}$$

where m_e^* is the electron effective mass in the conduction band and ε is the static dielectric constant. The quantity Ry^* can also be considered as an exciton binding energy.

Crucial for our consideration is the energy $V_{latt}(\Delta, \mathbf{r})$ that describes the reaction of the system to the ionization of Pr^{3+} into Pr^{4+}. $V_{latt}(\Delta, \mathbf{r})$ includes the electronic type energy related to ionization of an electron (delocalization of an electron) and the lattice relaxation energy, Δ being the shift of the ligands. In the adiabatic approximation one can consider the dependence on Δ and $\mathbf{r}$ in $V_{latt}(\Delta, \mathbf{r})$ separately:

$$V_{latt}(\Delta, \mathbf{r}) = V'_{latt}(\Delta) + V''_{latt}(\Delta, \mathbf{r}). \tag{3}$$

The decrease of the electron number alters the system energy by the quantity $-\frac{C}{R^m}$ (Gryk *et al* 2005b), where the exponent m depends on the model; $m = 1$ is for the classic electrostatic potential, $m = 2$ corresponds to the energy of an electron in a quantum well, $m = 5$ to the energy of an electron in a crystal field and $m = 12$ to inter-ionic repulsion given by the Lennard-Jones potential. Assuming $\frac{\Delta}{R} \ll 1$, one obtains

$$\Delta = -\frac{2C}{kR^{m+1}} \tag{4}$$

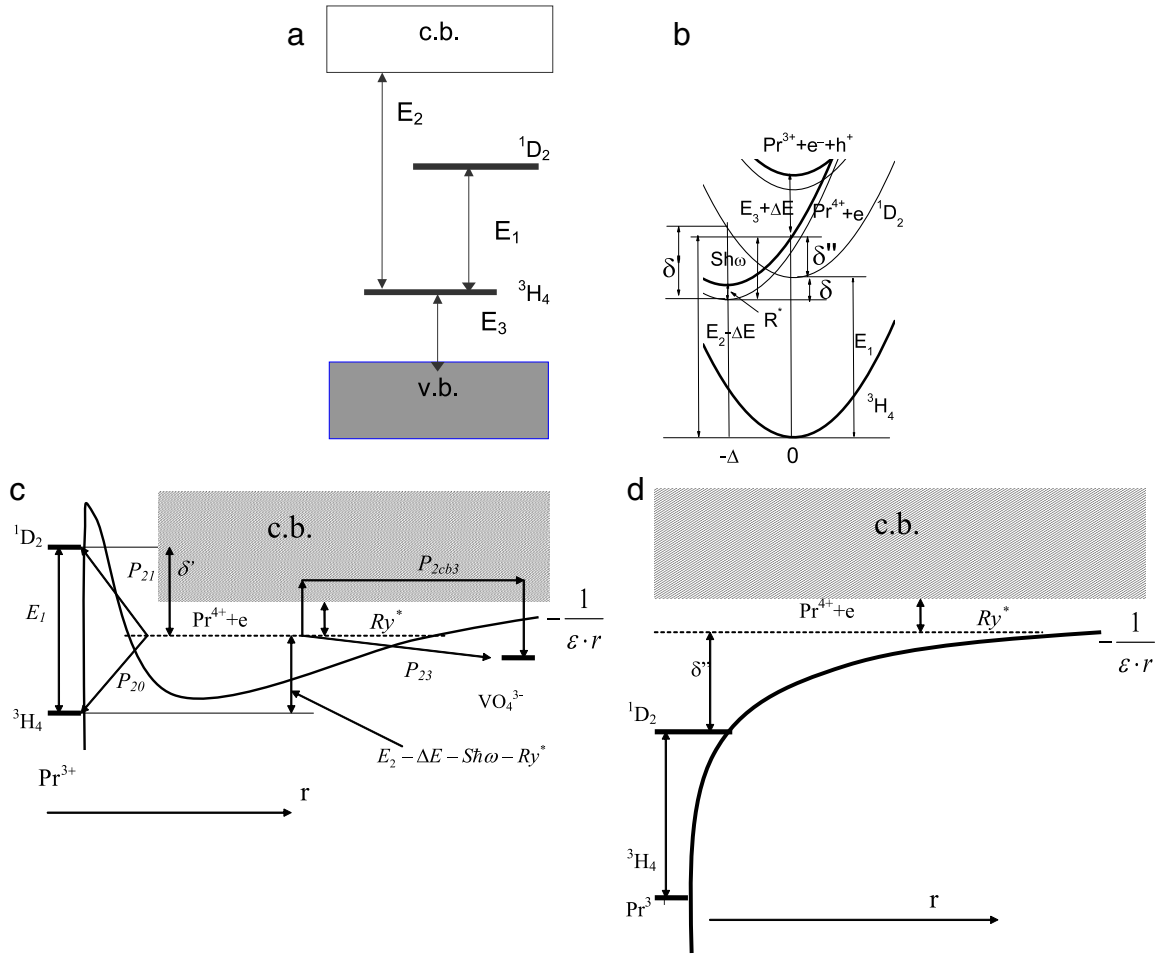

Figure 5. (a) Energy diagram of isovalent Pr^{3+} ion. (b) Configurational coordinate diagram representing the energetic structure of Pr^{3+} ion and trapped exciton system. (c) Realistic potential of Pr^{4+} system in presence of large lattice relaxation. (d) Realistic potential of Pr^{4+} system in absence of large lattice relaxation (rigid lattice approximation).

where k is the elastic constant of the material. Finally

$$V'_{\text{latt}}(\Delta) = -\Delta E - S\hbar\omega, \tag{5}$$

where $S\hbar\omega$ is the lattice relaxation energy:

$$S\hbar\omega = \frac{k}{2}(\Delta)^2 = \frac{2C^2}{kR^{2(m+1)}}, \tag{6}$$

and

$$\Delta E = \frac{C}{R^m}. \tag{7}$$

$V''_{\text{latt}}(\Delta, \mathbf{r})$ is the potential created by shifted ligands and is equal to

$$V''_{\text{latt}}(\Delta, \mathbf{r}) = \sum_i \frac{Z_i}{|\mathbf{r} - \mathbf{R}_i|^3}(\mathbf{r} - \mathbf{R}_i) \cdot \Delta_i. \tag{8}$$

Considering relations (1)–(7) one obtains the configurational coordinate diagram shown in figure 5(b). The lowest parabola corresponds to the $^3H_4$ ground state of the Pr^{3+} ion. The next parabola corresponds to the excited $^1D_2$ state separated from the ground state by the energy E_1. The upper parabola labeled $Pr^{3+} + e + h$ corresponds to the excited system: the Pr^{3+} ion in its ground state, and the free electron and hole in the conduction and valence band, respectively. The thin parabola below represents the free Frenkel type exciton. In semiconductors, where the effective masses of electrons and holes are well defined, its binding energy is equal to $R^*_{\text{ex}} = -13.6\frac{m^*_h m^*_e}{\varepsilon^2(m^*_e + m^*_h)}$ eV.

The parabolas labeled $Pr^{4+} + e$ represent Pr^{4+} (Pr^{3+} with a captured hole) and an electron in the conduction band (thick parabola) and Pr^{4+} and an electron captured by the Coulomb potential at a trapped exciton state (thin parabola). The trapped exciton states can be reached in two ways:

(i) The system is excited to the state $Pr^{3+} + e + h$, then the hole is trapped at the Pr^{3+} ion. This decreases the free electron–hole system energy by the quantity $E_3 + \Delta E$ and the electron–lattice relaxation energy $S\hbar\omega$.

(ii) The Pr^{3+} can by ionized directly by a photon with energy $E_2 - \Delta E$, then the system relaxes, decreasing its energy by $S\hbar\omega$. Then, either the electron is still in the conduction band or it is trapped by the Coulomb potential of the Pr^{4+} ion.

Pressure compresses the system (the ion–ligand distance R decreases). As a result the energy ΔE increases with

increasing pressure. On the other hand, changes in energy $S\hbar\omega$, defined by relation (6), are rather small (Grinberg 2006) because pressure causes a decrease of R and the increase of the elastic constant k. As a result one expects that the energy of a trapped exciton decreases with pressure with respect to the energy of the $^1D_2$ state. In figure 5(b) the trapped exciton energy is lower than that of the $^1D_2$ state of Pr^{3+} by the quantity δ. In YVO_4:Pr^{3+} such a situation occurs for pressures higher than 68 kbar.

To understand why at high pressure the luminescence of Pr^{3+} is replaced by the perturbed VO_4^{3-} luminescence one should consider the realistic potential which creates the energetic structure Pr^{4+} + e (Pr-trapped exciton) and Pr^{3+} ($^1D_2$, $^3H_4$ states) in the presence of strong lattice relaxation. The shifted ligands create the short range repulsion dipole-like potential given by the formula (8). Thus the actual potential seen by an electron in the conduction band is equal to

$$U(\mathbf{r}, \Delta) = V_{\mathrm{RE}}(\mathbf{r})|_{r<R} - \frac{e^2}{\varepsilon r} + V''_{\mathrm{latt}}(\Delta, \mathbf{r}). \tag{9}$$

In relation (9) the zero potential corresponds to the conduction band edge. The relation (8) presents the dipole-like potential. In order to visualize it, one can simplify the potential considering it as the one resulting from two charged spheres with radii R and $R - \Delta$, and charges $Q = \sum_i Z_i$ and $-Q$, respectively. Thus the potential $V''_{\mathrm{latt}}(\Delta, \mathbf{r}) = 0$ for $r > R$ and $r < R - \Delta$, and

$$V''_{\mathrm{latt}}(\Delta, \mathbf{r}) = V''_{\mathrm{latt}}(\Delta, r) = \frac{Q}{R^2}(R - r) \quad \text{for } R - \Delta < r < R. \tag{10}$$

The potential described by relation (9) with further simplifications is presented in figure 5(c). One notices that the potential (9) is centro-symmetrical and in figure 5(c) it is presented as a function of r (solid curve). The shaded box represents continuum states (the conduction band edge corresponds to the bottom of the box). At a large distance from Pr^{4+}, the potential $U(\mathbf{r}, \Delta)$ is equal to $-\frac{e^2}{\varepsilon r}$, whereas for a short distance from praseodymium the shifted ligands create the short range repulsion potential given by formula (8). For $r < R - \Delta$ we have the local potential of the Pr^{4+} ion that can bind the electron at the localized Pr^{3+} states. The dashed line represents the level that can be occupied by the electron captured by the Coulomb potential of Pr^{4+}. In figure 5(c) the binding energy of this state is labeled as Ry*, although it differs from the quantity given by relation (2), since the local potential differs from the Coulomb one. The thick solid lines represent the Pr^{3+} states $^1D_2$ and $^3H_4$. One notices that the potential created by the shifted ligands causes the increase of the energies of the $^1D_2$ and $^3H_4$ states of Pr^{3+} by a quantity approximately equal to $\frac{Q}{R^2}\Delta$. The shifted ligands create the energy barrier that separates the localized states of Pr^{3+} from the delocalized state of the type Pr^{4+} + e. The diagram presented in figure 5(c) corresponds to the energetic structure of the system with large lattice relaxation (for the configurational coordinate equal to $-\Delta$ in the diagram presented in figure 5(b)). When an electron is captured at the $^1D_2$ or $^3H_4$ states the repulsion potential (defined by (8)) related to the lattice distortion disappears and the energies of the $^1D_2$ and $^3H_4$ states are shifted down with respect to the conduction band (continuum states), which corresponds to the position '0' in the diagram in figure 5(b). The realistic potential without lattice relaxation is shown in figure 5(d).

To analyze the relaxation process of PTE one considers the nonradiative and radiative transitions in the system. The probability of nonradiative transition from the trapped exciton state (labeled 2) to the $^1D_2$ state (labeled 1) is given by

$$P_{21} = P_{21}^0 \exp\frac{-\delta}{kT}. \tag{11}$$

To calculate the quantity P_{21}^0 one should consider the configurational coordinate diagram in figure 5(b) and the Born–Oppenheimer functions $\Phi = \varphi(\mathbf{r}) \cdot \chi(\mathbf{R})$, where $\varphi(\mathbf{r})$ and $\chi(\mathbf{R})$ are electronic and vibrational wavefunctions, respectively. Thus

$$P_{21}^0 = \left| \int \varphi_2^*(\mathbf{r}) T \varphi_1(\mathbf{r})\, \mathrm{d}\mathbf{r} \right|^2 \cdot \left| \int \chi_2^{m*}(\mathbf{R}) \chi_1^0(\mathbf{r})\, \mathrm{d}\mathbf{R} \right|^2 \tag{12}$$

where T is the operator that allows a nonradiative transition and the superscript m at the vibrational wavefunction corresponds to the number of phonons that is needed for the Pr^{4+} + e system to reach the energy of the $^1D_2$ electronic manifold (diagram in figure 5(b)).

The transition from the PTE to the ground state $^3H_4$ of Pr^{3+} (labeled 0) is considered as a superposition of radiative and nonradiative processes. Thus the quantity P_{20} is given by

$$P_{20} = P_{\mathrm{rad}} + P_{\mathrm{nrad}} \tag{13}$$

where

$$P_{\mathrm{rad}} = \left| \int \varphi_2^*(\mathbf{r}) M \varphi_0(\mathbf{r})\, \mathrm{d}\mathbf{r} \right|^2 \cdot \sum_n \left| \int \chi_2^{0^*}(\mathbf{R}) \chi_0^n(\mathbf{r})\, \mathrm{d}\mathbf{R} \right|^2 \tag{14}$$

where M is the radiative transition moment. The summation over n represents transitions to all vibrational states of the ground electronic level $^3H_4$. The nonradiative transition takes place without changing the energy of the system from the state $\varphi_2(\mathbf{r}) \cdot \chi_2^0(\mathbf{R})$ to the state $\varphi_0(\mathbf{r}) \cdot \chi_0^n(\mathbf{R})$:

$$P_{\mathrm{nrad}} = \left| \int \varphi_2^*(\mathbf{r}) T \varphi_0(\mathbf{r})\, \mathrm{d}\mathbf{r} \right|^2 \cdot \left| \int \chi_2^{0^*}(\mathbf{R}) \chi_0^n(\mathbf{r})\, \mathrm{d}\mathbf{R} \right|^2. \tag{15}$$

One notices that the initial electronic wavefunction $\varphi_2(\mathbf{r})$ is the eigenfunction of the Hamiltonian with the potential presented in figure 5(c). Because of the large repulsion of short range potential of the shifted ligands, the probability of finding the electron in the core area of the Pr^{4+} is small ($|\varphi_2(\mathbf{r})|^2 \approx 0$), for $r < R$, whereas eigenfunctions $\varphi_1(\mathbf{r})$ and $\varphi_0(\mathbf{r})$ are localized at a distance from the ion much smaller than R. As a result, the quantities $|\int \varphi_2^*(\mathbf{r}) T \varphi_1(\mathbf{r})\, \mathrm{d}\mathbf{r}|^2$, $\int \varphi_2^*(\mathbf{r}) T \varphi_0(\mathbf{r})\, \mathrm{d}\mathbf{r}|^2$ and $\int \varphi_2^*(\mathbf{r}) M \varphi_0(\mathbf{r})\, \mathrm{d}\mathbf{r}|^2$ are close to zero. This gives rise to the fact that the quantities P_{21} and P_{20} (especially P_{20}) are smaller than the transitions between the states of the $4f^2$ electronic configuration of Pr^{3+}. The probability P_{21} is additionally decreased by an exponential factor (see relation (11)).

One should notice that the large lattice relaxation is related to the effect of ionization of praseodymium from Pr^{3+} to Pr^{4+} and is not affected by the fact that the electron is captured at the trapped exciton state $Pr^{4+} + e$, or not. In the latter case a large lattice relaxation can stabilize the Pr^{4+} system. Actually the electron trapped at the Pr^{4+} in a quasi-shallow donor state can be excited to the conduction band and can recombine at the VO_4^{3-} center with another hole. This process is described by the probability P_{2cb3}. Such a mechanism is preferred by the fact that the short range repulsion potential decreases the exciton binding energy Ry^*.

The effective Bohr radius of the electron at Pr^{4+} is equal to $a_0 \frac{\varepsilon}{m^*}$, where a_0 is the Bohr radius. For small effective mass and large dielectric constant, the probability of finding the electron decreases slowly with the distance from the Pr^{4+} and therefore the de-excitation pathway described by probability P_{23} can also be active.

Formally the conditions that are satisfied at high pressure can be expressed as follows:

$$P_{20}, P_{21} < P_{23} \tag{16}$$

and/or

$$P_{20}, P_{21} < P_{2cb3}. \tag{17}$$

Considering that for pressures greater than 50 kbar the energy δ' becomes positive and increases with increasing pressure, the probability P_{21} decreases with pressure quite rapidly. Pressure can decrease the value of P_{20} because it can cause an increase of the space separation between the electronic wavefunctions $\varphi_2(\mathbf{r})$ and $\varphi_0(\mathbf{r})$ since this separation increases when Δ increases with increasing pressure. The larger local repulsion potential also gives rise to an decrease of the binding energy of the trapped exciton Ry^* and an increase of the delocalization of the electron. As a consequence, the probabilities of decomposition of the trapped exciton, P_{23} and P_{2cb3}, can increase with increasing pressure.

5. Conclusions

It has been shown that, at high pressure, the quenching of the $^1D_2$ luminescence is accompanied by the recovering of the VO_4^{3-} luminescence. This means that at high pressure the Pr^{3+} ion in YVO_4 is no longer luminescent and cannot be considered any more as involved in nonradiative recombination of electrons and holes. This effect has been explained through the influence of pressure on the PTE state. Actually the pressure decreases the energy of the trapped exciton and causes the level crossing with the $^1D_2$ state of the Pr^{3+} ion. A model is developed for the trapped exciton, in which a hole is trapped at Pr^{3+} and an electron is bound by the long range Coulomb potential of Pr^{4+}. Specifically it has been shown that the pressure-induced recovering of the vanadate luminescence needs that the electron is bound at delocalized shallow donor-like states.

Acknowledgments

This paper has been supported by the Polish Ministry of Science and Higher Educations through a grant active in years 2008–2010.

References

Blasse G 1980 *Struct. Bond.* **42** 1
Boutinaud P, Mahiou R, Cavalli E and Bettinelli M 2004 *J. Appl. Phys.* **96** 4923
Boutinaud P, Mahiou R, Cavalli E and Bettinelli M 2006a *Chem. Phys. Lett.* **418** 185
Boutinaud P, Mahiou R, Cavalli E and Bettinelli M 2007 *J. Lumin.* **122/123** 430
Boutinaud P, Pinel E, Dubois M, Vink A P and Mahiou R 2005 *J. Lumin.* **111** 69
Boutinaud P, Pinel E, Oubaha M, Mahiou R, Cavalli E and Bettinelli M 2006b *Opt. Mater.* **28** 9
Grinberg M 2006 *Opt. Mater.* **28** 26
Grinberg M and Mahlik S 2008 *J. Non-Cryst. Solids* **354** 4163
Gryk W, Dujardin C, Joubert M-F, Ryba-Romanowski W, Malinowski M and Grinberg M 2006 *J. Phys.: Condens. Matter* **18** 117
Gryk W, Dyl D, Grinberg M and Malinowski M 2005a *Phys. Status Solidi* c **2** 188
Gryk W, Dyl D, Ryba-Romanowski W and Grinberg M 2005b *J. Phys.: Condens. Matter* **17** 5381
Gryk W, Kuklinski B, Grinberg M and Malinowski M 2004 *J. Alloys Compounds* **380** 230
Kubicki A A, Bojarski P, Grinberg M, Sadownik M and Kukliński B 2006 *Opt. Commun.* **269** 275
Koepke Cz, Wisniewski K, Dyl D, Grinberg M and Malinowski M 2006 *Opt. Mater.* **28** 137
Merrill L and Bassett W A 1974 *Rev. Sci. Instrum.* **45** 290
Polosan S, Bettinelli M and Tsuboi T 2007 *Phys. Status Solidi* c **4** 1352
Reut E G and Ryskin A I 1973 *Phys. Status Solidi* a **17** 47
Ryba-Romanowski W 2003 *Cryst. Res. Technol.* **38** 25